



Exploring sources of biogenic secondary organic aerosol compounds using chemical analysis and the FLEXPART model

Johan Martinsson^{1,2}, Guillaume Monteil³, Moa K. Sporre⁴, Anne Maria Kaldal Hansen⁵, Adam Kristensson¹, Kristina Eriksson Stenström¹, Erik Swietlicki¹, Marianne Glasius⁵

5 ¹Division of Nuclear Physics, Lund University, Box 118, SE-22100, Lund, Sweden

²Centre for Environmental and Climate Research, Lund University, Ecology Building, SE-22362, Lund, Sweden

³Department of Physical Geography, Lund University, Lund, Box 118, SE-22100, Lund, Sweden

⁴Department of Geosciences, University of Oslo, Postboks 1022, Blindern, 0315, Oslo, Norway

⁵Department of Chemistry and iNANO, Aarhus University, Langelandsgade 140, DK-8000, Aarhus C, Denmark

10 *Correspondence to:* Johan Martinsson (johan.martinsson@nuclear.lu.se)

Abstract. Molecular tracers in secondary organic aerosols (SOA) can provide information on origin of SOA, as well as regional scale processes involved in their formation. In this study nine carboxylic acids, eleven organosulfates (OSs) and two nitrooxy organosulfates (NOSs) were determined in daily aerosol particle filter samples from Vavihill measurement station in southern Sweden during June and July 2012. Several of the observed compounds are photo-oxidation products from biogenic volatile organic compounds (BVOCs). Highest average mass concentrations were observed for carboxylic acids derived from fatty acids and monoterpenes (12.3 ± 15.6 and 13.8 ± 11.6 ng/m³, respectively). The FLEXPART model was used to link 9 specific surface types to single measured compounds. It was found that the surface category “sea and ocean” was dominating the air mass exposure (54%) but contributed to low mass concentration of observed chemical compounds. A principal component (PC) analysis identified four components, where the one with highest explanatory power (49%) displayed clear impact of coniferous forest on measured mass concentration of a majority of the compounds. The three remaining PC’s were more difficult to interpret, although azelaic, suberic, and pimelic acid were closely related to each other but not to any clear surface category. Hence, future studies should aim to deduce the biogenic sources and surface category of these compounds. This study bridges micro level chemical speciation to air mass surface exposure on the macro level.

15
20



1 Introduction

Carbonaceous aerosols are abundant in ambient air around the world and account for 25% of the European PM₁₀ mass (Fuzzi et al., 2015). The carbonaceous aerosol fraction has severe effects on human health as well as a profound effect on the Earth climate system (Dockery et al., 1993; Pope et al., 1995). During summer, carbonaceous aerosols are mainly of biogenic origin, emitted either through primary emissions or gas-phase oxidation products from biogenic volatile organic compounds (BVOCs) (Genberg et al., 2011; Yttri et al., 2011). BVOCs are primarily emitted from plants as a tool for communication and to handle biotic and abiotic stress (Laothawornkitkul et al., 2009; Monson et al., 2013; Penuelas and Llusia, 2003; Sharkey et al., 2008). The emissions of BVOCs tend to increase with increasing temperature and photosynthetically active radiation (PAR) (Guenther et al., 1995; Guenther et al., 1993; Hakola et al., 2003). Four main compound categories dominate the global BVOCs emissions; isoprene (C₅H₈), monoterpenes (C₁₀H₁₆), other reactive VOCs and less reactive VOCs (Laothawornkitkul et al., 2009). Isoprene is emitted from a variety of plants, however mainly from deciduous forests and shrubs which may account for more than 70% of the emissions (Guenther et al., 2006). Monoterpenes are largely emitted from coniferous trees like pine and spruce, but also from some deciduous trees, such as birch (Mentel et al., 2009). The most abundant monoterpenes in the boreal forests include α -pinene, β -pinene and limonene (Hakola et al., 2012).

Biogenic secondary organic aerosols (BSOA) are formed by photo-oxidation of BVOCs, a process which tends to lower the saturation vapor pressure of the oxidation products relative to that of the BVOCs, thus forcing the gas phase products to partition into the aerosol-phase. BSOA has been shown to dominate over combustion source aerosols during summer (Genberg et al., 2011; Yttri et al., 2011). Yttri et al. (2011) performed source apportionment at four sites in Scandinavia during August 2009 and found that the biogenic contribution to the carbonaceous aerosol dominated (69-86%) at all four sites. Genberg et al. (2011) performed a one year source apportionment at one site in southern Sweden where they apportioned 80% of the summer-time carbonaceous aerosol to biogenic sources. Gelencser et al. (2007) also reported biogenic source dominance (63-76%) of the carbonaceous aerosol at 6 sites in south-central Europe during summer. Castro et al. (1999) observed a maximum and minimum in SOA in Europe during summer and winter, respectively. The relative SOA contribution was higher in rural forest and ocean measurement sites compared to urban sites (Castro et al., 1999).

BSOA consists of a myriad of organic compounds. Small (carbon number: C₃-C₆) and larger (C₇-C₉) dicarboxylic acids are highly hydrophilic and hygroscopic which have shown to result in potential strong climate effect due to their cloud condensation properties (Cruz and Pandis, 1998; Kerminen, 2001). Dicarboxylic acid contribution to carbon mass has been estimated to 1-3% in urban and semi-urban areas and up to 10% in remote marine areas (Kawamura and Ikushima, 1993; Kawamura and Sakaguchi, 1999). Primary aerosol sources of dicarboxylic acids in atmospheric aerosols include ocean emissions, engine exhausts and biomass burning (Kawamura and Kaplan, 1987; Kundu et al., 2010; Mochida et al., 2003). However, the main source of dicarboxylic acids are oxidation/photo-oxidation processes of VOCs (Zhang et al., 2010). These VOC precursors may originate from both anthropogenic and biogenic sources (Mochida et al., 2003). However,



BVOCs constitute more than 50% of all atmospheric VOCs, which is approximately equal to 1150 Tg carbon y^{-1} (Guenther et al., 1995; Hallquist et al., 2009).

Organosulfates (OSs) and nitrooxy organosulfates (NOSs) are low volatility SOA products that in recent years have gained increased attention due to their potential properties as tracers for atmospheric ageing of aerosols in polluted air masses (Hansen et al., 2015; Hansen et al., 2014; Kristensen, 2014; Kristensen and Glasius, 2011; Nguyen et al., 2014). Many of these compounds are formed from isoprene and monoterpene oxidation products that react with sulfuric acid in the aerosol phase (Iinuma et al., 2007; Surratt et al., 2010; Surratt et al., 2007b). Since atmospheric sulfuric acid is mainly of anthropogenic origin (Zhang et al., 2009), presence of OSs from biogenic organic precursors thus indicates an effect of anthropogenic enhancement of BSOA (Hansen et al., 2014). Recently, OSs from anthropogenic organic precursors such as alkanes and PAHs have also been discovered (Riva et al., 2016; Riva et al., 2015). Tolocka and Turpin (2012) estimated that OSs could comprise up to 10% of the total organic aerosol mass in the U.S.

Many carboxylic acids and OSs originate from biogenic sources, however, the exact vegetation types emitting the precursor are poorly explored (Mochida et al., 2003; Tolocka and Turpin, 2012). Coniferous forests, deciduous forests, arable land, pastures etc. are all examples of potential BVOCs sources. Information on specific land surface type BVOCs and BSOA emissions is potentially crucial if an increased understanding should be reached on how land-use changes will affect organic aerosol levels and composition. Yttri et al. (2011) measured one dicarboxylic acid (pinic acid), four OSs and two NOSs at four locations in Scandinavia and connected this measurement data to the FLEXPART model (Stohl et al., 2005) footprint of specific surface landscape types. They used thirteen types of surface landscapes and found that the two NOSs (MW 295 and MW 297, both formed from monoterpenes) correlated with air mass exposure to mixed forest (Yttri et al., 2011).

In this study, a comprehensive measurement campaign was conducted in order to investigate sources and levels of BSOA. 38 sequential 24h filter samples were analyzed for 9 species of carboxylic acids, 11 species of OSs and 2 species of NOSs at a rural background station in southern Sweden. FLEXPART model simulations at the time and location of the observations were then used to estimate the potential origin of the aerosols sampled.

2 Methods

2.1 Location and sampling

The Vavihill measurement station is a rural background station in southern Sweden (56°01' N, 13°09' E, 172 m.a.s.l.) within EUSAAR (European Supersites for Atmospheric Aerosol Research) and EMEP (European Monitoring and Evaluation Programme). The surrounding landscape consists of pastures, mixed forest and arable land. The largest nearby cities are Helsingborg (140 000 inhabitants), Malmö (270 000 inhabitants) and Copenhagen (1 990 000 inhabitants) at a distance of 25, 45 and 50 km, respectively. These cities are in the west and southwest direction from the measurement station. Previous observations have shown that air masses from continental Europe are usually more polluted than air masses from the north and westerly direction, i.e. Norwegian Sea and Atlantic Ocean (Kristensson et al., 2008).



38 filter samples of aerosols were collected at the Vavihill field station in southern Sweden from 10th of June to 18th of July 2012. Aerosols were collected on 150 mm quartz fibre filters (Advantec) using a high volume sampler (Digitel, DHA-80) with a PM₁ inlet. The filters were heated to 900°C for four hours prior to sampling, with the purpose of removing adsorbed organic compounds from the filters. The sampling air flow was 530 litres per minute and total sampling time per filter was 24 hours. Sampled filters were wrapped in aluminium foil and stored at -18°C until extraction.

2.2 BSOA analysis

The method for extraction and analysis is based on previous studies (Hansen et al., 2014; Kristensen and Glasius, 2011; Nguyen et al., 2014) and thus only described briefly here. For extraction each filter was placed in a beaker and spiked with 15 µl of a 100 µg/ml recovery standard (camphoric acid). The filter was covered with 90% acetonitrile with 10% MilliQ water and extracted in a cooled ultrasound bath for 30 min. The extract was filtered through a Teflon filter (0.45 µm pore size, Chromafil) and evaporated until dryness using a rotary evaporator. The sample was then re-dissolved twice in 0.5 ml 3% acetonitrile, 0.1% acetic acid, and stored in a refrigerator (3-5°C) until analysis. The samples were analysed with an Ultra High Performance Liquid Chromatograph (UHPLC, Dionex) coupled to a quadrupole Time-Of-Flight Mass Spectrometer (q-TOF-MS, Bruker Daltonics) through an electro-spray ionisation (ESI) inlet. The UHPLC stationary phase was an Acquity T3 1.8 µm (2.1 × 100 mm) column from Waters, and the mobile phase consisted of eluent A: 0.1% acetic acid and eluent B: Acetonitrile with 0.1% acetic acid. The operational eluent flow was 0.3 mL/min and an 18 min. multistep gradient was applied: From 1 min. to 10 min. eluent B increased from 3% to 30%, then eluent B increased to 90% during 1 min, where it was held for 1 min, before eluent B was increased further to 95% (during 0.5 min) kept here for 3.5 min. before reduction to 3% (during 0.5 min) for the remaining 0.5 min of the analysis. The ESI-q-TOF-MS was operated in negative ionisation mode with a nebulizer pressure of 3.0 bar and a dry gas flow of 8 L/min. All data were acquired and processed using Bruker Compass software. The analyzed dicarboxylic acids, OSs and NOSs are summarized in Table 1 and 2, respectively. Authentic standards were used for identification and quantification of all carboxylic acids, while OSs and NOSs were identified based on their MS/MS loss of HSO₄⁻ (m/z = 97) and an additional neutral loss of HNO₃ (m/z = 63) in the case of NOSs. This work focused on identification of OSs from biogenic organic precursors, since OSs from alkanes and PAHs had not been discovered at the time of the analysis. OSs and NOSs were quantified using surrogate standards of OS 250 derived from β-pinene (synthesized in-house), octyl sulfate sodium salt (≥95% Sigma-Aldrich) or D-mannose-6-sulfate sodium salt (≥90% Sigma-Aldrich) based on their retention times in the UHPLC-q-TOF-MS system (Table 2). A linear or quadratic relationship between peak area and concentration was demonstrated for all standards and surrogates, and the correlation coefficients, R², of all calibration curves were better than 0.98 (n = 7 data points). The analytical uncertainty was estimated to be <20% for carboxylic acids and <25% for OSs and NOSs. The uncertainty of the absolute concentrations of OSs and NOSs are higher than carboxylic acids due to lack of authentic standards.

2.3 Auxiliary measurements and analysis



PM_{2.5} was measured with one hour time resolution using a tapered element oscillating microbalance (TEOM, Thermo, 8500 FDMS), and estimated uncertainty was less than 25%. Geographical air mass origin was analyzed with the Hybrid Single Particle Lagrangian Integrated Trajectory Model (HYSPLIT) model (Draxier and Hess, 1998; Stein et al., 2015). Gridded meteorological data from the Centre of Environmental Predictions (NCEP) Global Data Assimilation System (GDAS) were used as input by the trajectory model. Back-trajectories were calculated at an hourly frequency 120-hour backward in time and the trajectories started 100 m above ground at the Vavihill measurement site. For each filter sample, 24 trajectories were used since the sampling time was 24 hours.

2.4 Source apportionment

The concentration and chemical composition of an aerosol sample depends on the trajectory of the sampled air mass in the days preceding the observation (whether or not it gets in contact with a source of aerosols or of aerosol precursors), but also on other meteorological factors such as the temperature and the amount of solar radiation (which control the chemical reactions that lead to production, destruction and transformation of aerosols), and the occurrence of precipitations, which can lead to a rapid scavenging of aerosol particles. A formal source apportionment would require a precise accounting of these factors, which is extremely complicated and is clearly out of the scope of this study. We can however already obtain valuable information just by looking at the trajectories of the air masses, and in particular, by estimating how much the air has been exposed to each land surface type.

We used the FLEXPART Lagrangian particle dispersion model in its version 10.0 (Seibert and Frank, 2004; Stohl et al., 2005) to compute seven days backward footprints for each observation. The principle is that, for each observation, FLEXPART computes the dispersion backward in time of a large number of “particles” (i.e. small virtual air masses). A 4D (space/time) domain is defined, and the aggregated residence time of the particles in each grid box of that domain represents the sensitivity of the observation to processes within that grid box. The temporal domain is hourly (from the release of the particles to seven days before), and the spatial domain is a 0.2°x0.2° grid, ranging from 30°N to 65°N and from 2°W to 32°E. Only one surface vertical level was used, ranging from the surface to a threshold altitude level, defined as half of the boundary layer height (computed by FLEXPART for each particle at each time step). This choice of a single surface layer means that the observations are considered insensitive to aerosol production/destruction above that layer. Accounting for such non-linear processes would require a more complex knowledge of the aerosol chemistry, and probably a more complex numerical model. The implications for this approximation are discussed in results and discussion section.

One footprint was computed for each observation, based on the dispersion seven days backward in time of 100000 FLEXPART particles. Default parameters for the FLEXPART “AERO-TRACER” tracer were used (i.e. dry and wet deposition schemes account for the removal of aerosols from the atmosphere by gravitational settling and rain washout). FLEXPART configuration files are provided in Supplementary Information.

To compute the exposure of each sample to different land surface types, we coupled the information from the footprints to the CORINE 2012 land cover map (Copernicus, 2012). CORINE 2012 is a high resolution (250x250m) map of the land



surface types in the European Union (44 land surface categories, to which we added a “sea and cean” category). The exposure E_i of one observation to the land type i is given by $E_i = \sum_j f_j^i R_j$, where j is one pixel of the domain, f_j^i is the fraction of the land surface type i in that pixel, and R_j is the sensitivity of the observation to that pixel (i.e. the value of the footprint at that location).

- 5 It is important to remember that since non-linear processes are not accounted for by the FLEXPART simulations, these land surface exposures are not a proper source apportionment, but are only a tool to interpret the observations.

2.5 Principal Component Analysis (PCA)

In order to deduce potential sources of measured BSOA compounds a principal component analysis (PCA) was performed
10 on measured chemical compounds together with air mass exposure to the landscape surface types derived from the FLEXPART model. The principle of PCA is that if measured parameters from the same source are strongly correlated they are treated as one principal component (PC), i.e. PCA identifies variables that have a prominent role by analysis of correlation and variance. PCA were performed by using the software SPSS (version 23, IBM).

15 3 Results and discussion

3.1 Variations and features in BSOA compounds

A total of 9 organic acids, 11 OSs and 2 NOSs of anthropogenic and biogenic origin were determined in the samples (Tables 1 and 2). All organic acids were quantified with authentic standards whereas the other compounds were quantified with surrogates (see experimental section). On average, the total mass of the organic chemical species from filters contributed to
20 0.3% ($\pm 0.2\%$, standard deviation) to $PM_{2.5}$. However, it is worth noticing that the particles were sampled through a PM_1 inlet, which most probably has excluded a considerable portion of the mass collected on filters compared to the $PM_{2.5}$ mass measured by the TEOM. On the other hand, it has been shown that PM_1 can comprise up to 90% of $PM_{2.5}$ in rural locations during summertime (Gomiscek et al., 2004). Since no gravimetric analysis of filters was performed, no information on the total mass loading of PM_1 is available.

25 In Table 3 and Fig. 1A concentrations of observed compounds during the sampling period are given. The compounds have been merged into groups based on their likely precursors in Fig. 1A (see Tables 1 and 2). Table 3 summarizes concentration ranges, means and standard deviations (SDs) for individual dicarboxylic acids, OSs and NOSs. In general the organic acids from monoterpenes and fatty acids dominate the total concentration over the entire period, where the concentration of acids from monoterpenes range from 1.7 to 49.0 $ng\ m^{-3}$ and the concentration of organic acids from fatty acids range from 0.03 to
30 64.1 $ng\ m^{-3}$. The concentration of isoprene-derived OSs ranges from 0.34 to 21.6 $ng\ m^{-3}$ over the sampling period and dominates over the monoterpene-derived OSs. This pattern has also been observed in other studies in the Nordic countries (Yttri et al., 2011), and is in line with high emissions of isoprene during summer. The NOSs are low in average concentration (NOS 295=0.12 \pm 0.11 ng/m^3 , NOS 297=0.05 \pm 0.03 ng/m^3), and are lower than the observed mean



concentration by Yttri et al. (2011) from the summer of 2011 (NOS 295=0.74 ng/m³, NOS 297=1.2 ng/m³). This could be due to differences in aerosol sources and surrogate standards for quantification between the two studies.

The fatty acid derived azelaic acid was found to be the most abundant dicarboxylic acid with a concentration range from 0.03 to 55.3 ng/m³ (mean=10.5±13.8 ng/m³). Hyder et al. (2012) who measured 9 dicarboxylic acids in aerosol samples obtained at the Vavihill measurement station 2008-2009 also found azelaic acid to be the most prominent with peak concentration during summer (16.2 ng/m³). The concentration of the anthropogenic acids is low (mean≈2 ng/m³) except during the 27th of June and the 6th of July when the concentration reaches 19.6 and 16.0 ng/m³, respectively. The spike in concentration of anthropogenic acids during these two days is caused by an increase in the concentration of adipic acid.

Correlations between the different compounds was investigated by Pearson correlation. All Pearson r-coefficients are given in Table 4. In general, the biogenic compounds (derived from isoprene and monoterpenes) correlated well ($r \geq 0.8$) with each other. The only exception was OS 250, which showed low to medium correlation with the other compounds.

Three dicarboxylic acids (azelaic, pimelic and suberic acid) correlated well with each other ($r > 0.87$). It is likely that the fatty acid derived dicarboxylic acids has a different origin than isoprene and monoterpene generated acids, a conclusion that also was reached in a previous study (Hyder et al., 2012). It was expected that adipic acid would show good agreement with pimelic acid since they are both suggested to be of anthropogenic origin. However, this correlation was poor ($r = 0.16$) and is believed to be explained by two strong concentration peaks in adipic acid (27th of June and 6th of July, Fig. 1A) with no corresponding peak in pimelic acid.

3.2 Air mass surface exposure

Figure 1B displays the exposures of the samples to the nine largest surface categories as percentage contribution and Tables 5 and 6 present the mean exposures and a correlation matrix for the investigated surface types. These surface categories are explained in more detail in the supplemental information. The “sea and ocean” category is dominating the exposure with an average of 56% (±16%). This is hardly surprising since a majority of the incoming air mass is from the westerly region where the North Atlantic Ocean, North Sea and Norwegian Sea are situated. The second most common surface exposure is from “non-irrigated arable land” (mean=19% ±8%). This is a common land type in continental Europe which is anti-correlated ($r = -0.84$) to the “sea and ocean” surface category. The fact that several land-based surface categories anti-correlated to the “sea and ocean” category may be an indicator of the model working properly. The category “other” has a significant contribution to the total exposure (mean=8% ±3%), but it groups 34 surface categories and is therefore difficult to interpret beyond the common fact that all these categories are land masses. It is important to remember that these exposures should not be read as a representation of the contribution of the land surface types to the production of the aerosols measured. For that, an estimation of the aerosol production (or transformation) associated to each surface category would be required. However, correlating the land surface exposures to the measured aerosol time series can provide an indication on the origin of the aerosols.



During a period of increased concentrations of molecular BSOA compounds (6th to 8th of July) the air mass was more exposed to land surface categories such as “non-irrigated arable land”, “coniferous forest”, “broad leaved forest” and “pastures” on the expense of “sea and ocean” (Fig. 1A-B). Further, the category “other” is also increased during this particular period. Within the “other” category, “mixed forest”, “complex cultivation patterns”, “land principally occupied by agriculture, with significant areas of natural vegetation” and “transitional woodland/shrub” are dominating (more information about the surface categories can be found on the CORINE database homepage) (EEA, 2016). This particular concentration increase is caused by the fatty acid-derived organic acids, monoterpene-derived organic acids and isoprene-derived OSs (Fig. 1A). The concentration of PM_{2.5} does not provide any explanation of the cause of the high concentrations, since PM_{2.5} is in general high during the entire campaign period. Both the HYSPLIT and FLEXPART model revealed that arriving air masses during this period mainly had an origin from continental Europe (Fig. 2). As stated earlier, it has been observed that air masses arriving from this direction usually carry more PM and OSs than from other directions (Nguyen et al., 2014; Kristensson et al., 2008).

The period of increased concentrations of molecular BSOA compounds (6th to 8th of July) are in large contrast to the “clean periods” observed during 12th-16th of June and 16th-18th of July (Fig. 1A-B). In particular, the latter period shows very low values of molecular BSOA compounds and a corresponding “sea and ocean” exposure of 79-86%. Hence, “sea and ocean” exposure does not seem to contribute to the measured mass of molecular BSOA compounds. Similarly, the “non-irrigated arable land” contributes to a significant fraction during 16th-18th of July (8-12%) and most probably does not contribute to the mass of measured BSOA species either.

3.3 Connection between surface type and measured species

To further investigate the impact of surface types on measured BSOA species a principal component analysis (PCA) was conducted as described in the method section. To our knowledge, the measured SOA species are derived from four possible precursor sources: anthropogenic, fatty acids, isoprene and monoterpene (Tables 1 and 2), hence a 4 PC VARIMAX-rotated solution was chosen. This solution explained 80.3% of the total variance. Table 7 shows the individual parameter contribution to the respective PC. PC1 accounts for 49.1% of the total variance and has strong positive contributions from several of the monoterpene derived dicarboxylic acids and both monoterpene and isoprene derived OSs and NOSs. The strongest positive surface category in PC1 is “coniferous forest”, suggesting that the species with a bold number in PC1 within Table 7 are originating, or that their mass concentration have a positive response, from coniferous forest. Coniferous forests are mainly known as large-scale emitters of monoterpenes. Despite this, the PCA illustrates that isoprene oxidation products are positively correlated to this surface category. Steinbrecher et al. (1999) observed negligible emissions of isoprene from common conifers as Scots pine (*Pinus sylvestris*) and common juniper (*Juniperus communis*). However, they found significant emissions from Norway spruce (*Picea abies*) which may explain some of the isoprene derived compounds in this study. Although the less strong positive contribution of 0.53, isoprene emitting “broad leaved forest” may also have contributed to the above described pattern in PC1.



PC2 accounts for 14.9% of the total variation and can roughly be classified as surface categories with low contribution to measured BSOA compounds. Six of the ten investigated surface categories show strong positive contribution to PC2 while many of the measured compounds show low and in some cases negative contribution to PC2. The observed pattern of high “sea and ocean” and “non-irrigated arable land” exposure when the mass concentration of BSOA compounds was low, further strengthens the explanation of PC2.

PC3 accounts for 9.3% of the total variance. The main contributors are suberic acid, azelaic acid and pimelic acid. They are all similar in chemical structure, although suberic and azelaic acid probably originate from fatty acids while pimelic acid likely is of anthropogenic origin (Table 1). Further, azelaic acid has been found to be involved in the triggering of the plant immune system (Jung et al., 2009). Hyder et al. (2012), who also found these three acids to be highly correlated in ambient aerosol, inferred that pimelic acid was either produced from the same source as suberic and azelaic acid or that pimelic acid is produced by continued oxidation of suberic and azelaic acid down to lower carbon numbered acids. None of the land surface categories displayed high contribution to PC3: “broad leaved forest” had the highest contribution of 0.21 while the other forest category, “conifer forest”, had a one order of magnitude lower contribution of -0.04. Hence, it is possible that broad leaved forests are more important for higher carbon (C7-C9) carboxylic acid production than coniferous forests.

PC4 accounted for 6.9% of the total variance and is harder to interpret than the previous three PC’s. The anthropogenic derived adipic acid has a positive PC contribution (0.59) as well as the surface categories “sparsely vegetated areas” (0.86) and “moors and heath” (0.85). The used land cover maps reveals that both “sparsely vegetated areas” and “moors and heath” are mainly found in Norway and northern Sweden, i.e. in the north and north-westerly direction of Vavihill measurement station. The overall interpretation of PC4 is difficult since adipic acid are thought to be of anthropogenic origin but, in this case, seem to correlate with landscape surface types that are sparsely populated and are associated with low human activity (i.e. “sparsely vegetated areas” and “moors and heath”). It is questionable whether the pre-assumed anthropogenic acids, adipic and pimelic acid, actually share any kind of origin since neither this study nor the study by Hyder et al. (2012) found any strong correlation between these two dicarboxylic acids. Nevertheless, future studies should repeat the presented methodology to focus on heavy anthropogenic influenced surface categories (i.e. cities, industries etc.) and their impact on anthropogenic acids and newly discovered anthropogenic OSs (Riva et al., 2016; Riva et al., 2015).

3.4 Uncertainties and limits

In this study, our analysis approach relies on two steps: first the calculation of the exposures, using FLEXPART, and then the estimation of land type contributions using a PCA analysis. Both steps suffer from uncertainties which limit the robustness of our results:

The longer the back-trajectories used in FLEXPART, the larger the error is likely to be. On the other hand, shorter back-trajectories lead to neglecting a larger proportion of “older” aerosols. We tested the impact of the footprint length choice on the exposure time series by repeating the analysis with footprints of 3 and 5 days (instead of 7 days in our default setup).



Overall, the exposures are not significantly affected, except for the exposure to the “sea and ocean” surface type during the 8-10 July peak, which show an uncertainty of 6% (Fig. S1).

The calculation of the observation exposures is based on the assumption that the measured aerosol compositions scale linearly with the aerosol production within the back-plume of the observation. This is not the case in reality: processes such as coagulation, nucleation, chemical reactions between aerosols and surrounding reactive gas species, photo-dissociation and wet and dry deposition (removal of aerosols from the atmosphere by the rain and by gravitational settling) alter the aerosol composition and concentration all along the air mass trajectory. Our approach also ignores the influence of aerosol particles (or precursors) older than seven days on the observations. Accounting adequately for all these processes would require a comprehensive (much heavier) aerosol model, which is totally out of the scope of this study. This mainly means that our approach cannot be used to quantify the aerosol production associated to, for example, a specific forest type. It nonetheless provides valuable qualitative information that could probably not be obtained with simpler single air-mass trajectory analysis such as the ones computed with the HYSPLIT model (Fig. 2).

The main limit to the PCA analysis is the shortness of the time series. In particular, there is only one strong event during the campaign (6-8 July), which is not enough for drawing strong conclusions. Our study can however be regarded as a proof-of-concept: computing FLEXPART footprints is relatively easy and lightweight, and could be performed routinely. The conclusions of a PCA analysis are likely to be a lot more robust with longer time series, and/or multi-sites observation campaigns (provided that the footprints of the different sites overlap sufficiently).

4 Conclusions

Nine carboxylic acids along with eleven organosulfates (OSs) and two nitrooxy organosulfates (NOSs) were analyzed from 38 daily aerosol samples sampled at Vavihill measurement station in southern Sweden during June and July 2012. Most of the measured compounds can be considered as photo-oxidation products from biogenic volatile organic compounds (BVOCs), hence derived from terrestrial plants. The FLEXPART model was used to identify exposure of the aerosol samples to several different surface categories. For easier interpretation, the study was focused on four potential source-specific components using 22 chemical species and the nine largest surface categories. The “sea and ocean” category was found to dominate the exposure, and other important categories were “non-irrigated arable land” and “pastures”. A principal component analysis (PCA) of four principal components (PC) was used to explore the impact and connection of surface categories on mass concentration of measured biogenic secondary organic aerosol compounds. It was found that coniferous forest had a positive effect on several of the measured monoterpene-derived compounds. The remaining three PCs were harder to interpret, however future studies should aim to investigate the sources of azelaic, suberic and pimelic acids which dominate in mass concentration but showed no clear correlation to surface categories.

This study demonstrates the interest of using an atmospheric transport model in aerosol source apportionment on specific chemical compounds. With the presented methodology it is possible to connect single chemical tracer compounds to potential local and long range aerosol sources, i.e. surface categories. Further, this FLEXPART application enables detailed



investigations on how natural and anthropogenic land-use changes may affect the mass concentration and chemical composition of ambient aerosol.

5 Data availability

- 5 All data are accessible through the supporting information.

Author contribution

- Johan Martinsson designed the study, compiled all data, performed the PCA and wrote most of the paper. Guillaume Monteil ran the FLEXPART simulations. Moa K. Sporre ran the HYSPLIT simulations. Anne Maria Kaldal Hansen and Marianne
10 Glasius ran the chemical analysis. Adam Kristensson, Erik Swietlicki and Kristina Eriksson Stenström assisted in the writing process.

Acknowledgements

This work was supported by the Swedish Research Council FORMAS (project 2011-743).

15

References

- Castro, L. M., Pio, C. A., Harrison, R. M., and Smith, D. J. T.: Carbonaceous aerosol in urban and rural European atmospheres: estimation of secondary organic carbon concentrations, *Atmos. Environ.*, 33, 2771-2781, Doi 10.1016/S1352-2310(98)00331-8, 1999.
- 20 Claeys, M., Iinuma, Y., Szmigielski, R., Surratt, J. D., Blockhuys, F., Van Alsenoy, C., Boge, O., Sierau, B., Gomez-Gonzalez, Y., Vermeylen, R., Van der Veken, P., Shahgholi, M., Chan, A. W. H., Herrmann, H., Seinfeld, J. H., and Maenhaut, W.: Terpenylic Acid and Related Compounds from the Oxidation of alpha-Pinene: Implications for New Particle Formation and Growth above Forests, *Environ. Sci. Technol.*, 43, 6976-6982, 10.1021/es9007596, 2009.
- 25 Copernicus Land Monitoring Services: <http://land.copernicus.eu/pan-european/corine-land-cover/clc-2012>, 2012.
- Cruz, C. N., and Pandis, S. N.: The effect of organic coatings on the cloud condensation nuclei activation of inorganic atmospheric aerosol, *J. Geophys. Res.-Atmos.*, 103, 13111-13123, Doi 10.1029/98jd00979, 1998.
- 30 Dockery, D. W., Pope, C. A., Xu, X. P., Spengler, J. D., Ware, J. H., Fay, M. E., Ferris, B. G., and Speizer, F. E.: An Association between Air-Pollution and Mortality in 6 United-States Cities, *New Engl. J. Med.*, 329, 1753-1759, Doi 10.1056/Nejm199312093292401, 1993.
- Draxier, R. R., and Hess, G. D.: An overview of the HYSPLIT_4 modelling system for trajectories, dispersion and deposition, *Aust. Meteorol. Mag.*, 47, 295-308, 1998.
- 35 List of Corine Reports: <http://www.eea.europa.eu/publications/COR0-part2/page001.html>, 2016.
- Fuzzi, S., Baltensperger, U., Carslaw, K., Decesari, S., van Der Gon, H. D., Facchini, M. C., Fowler, D., Koren, I., Langford, B., Lohmann, U., Nemitz, E., Pandis, S., Riipinen, I., Rudich, Y., Schaap, M., Slowik, J. G., Spracklen, D. V., Vignati, E., Wild, M.,
40 Williams, M., and Gilardoni, S.: Particulate matter, air quality and climate: lessons learned and future needs, *Atmos. Chem. Phys.*, 15, 8217-8299, 10.5194/acp-15-8217-2015, 2015.
- Gelencser, A., May, B., Simpson, D., Sanchez-Ochoa, A., Kasper-Giebl, A., Puxbaum, H., Caseiro, A., Pio, C., and Legrand, M.: Source apportionment of PM_{2.5} organic aerosol over Europe: Primary/secondary, natural/anthropogenic, and fossil/biogenic origin, *J. Geophys. Res.-Atmos.*, 112, Artn D23s0410.1029/2006jd008094, 2007.
- 45



- Genberg, J., Hyder, M., Stenstrom, K., Bergstrom, R., Simpson, D., Fors, E. O., Jonsson, J. A., and Swietlicki, E.: Source apportionment of carbonaceous aerosol in southern Sweden, *Atmos. Chem. Phys.*, 11, 11387-11400, 10.5194/acp-11-11387-2011, 2011.
- 5 Gomez-Gonzalez, Y., Surratt, J. D., Cuyckens, F., Szmigielski, R., Vermeylen, R., Jaoui, M., Lewandowski, M., Offenberg, J. H., Kleindienst, T. E., Edney, E. O., Blockhuys, F., Van Alsenoy, C., Maenhaut, W., and Claeys, M.: Characterization of organosulfates from the photooxidation of isoprene and unsaturated fatty acids in ambient aerosol using liquid chromatography/(-) electrospray ionization mass spectrometry, *J. Mass. Spectrom.*, 43, 371-382, 10.1002/jms.1329, 2008.
- 10 Gomiscek, B., Hauck, H., Stopper, S., and Preining, O.: Spatial and temporal variations Of PM1, PM2.5, PM10 and particle number concentration during the AUPHEP-project, *Atmos. Environ.*, 38, 3917-3934, 10.1016/j.atmosenv.2004.03.056, 2004.
- Guenther, A., Hewitt, C. N., Erickson, D., Fall, R., Geron, C., Graedel, T., Harley, P., Klinger, L., Lerdau, M., McKay, W. A., Pierce, T., Scholes, B., Steinbrecher, R., Tallamraju, R., Taylor, J., and Zimmerman, P.: A Global-Model of Natural Volatile Organic-Compound Emissions, *J. Geophys. Res.-Atmos.*, 100, 8873-8892, Doi 10.1029/94jd02950, 1995.
- 15 Guenther, A., Karl, T., Harley, P., Wiedinmyer, C., Palmer, P. I., and Geron, C.: Estimates of global terrestrial isoprene emissions using MEGAN (Model of Emissions of Gases and Aerosols from Nature), *Atmos. Chem. Phys.*, 6, 3181-3210, 2006.
- 20 Guenther, A. B., Zimmerman, P. R., Harley, P. C., Monson, R. K., and Fall, R.: Isoprene and Monoterpene Emission Rate Variability - Model Evaluations and Sensitivity Analyses, *J. Geophys. Res.-Atmos.*, 98, 12609-12617, Doi 10.1029/93jd00527, 1993.
- Hakola, H., Tarvainen, V., Laurila, T., Hiltunen, V., Hellen, H., and Keronen, P.: Seasonal variation of VOC concentrations above a boreal coniferous forest, *Atmos. Environ.*, 37, 1623-1634, 10.1016/S1352-2310(03)00014-1, 2003.
- 25 Hakola, H., Hellen, H., Hemmila, M., Rinne, J., and Kulmala, M.: In situ measurements of volatile organic compounds in a boreal forest, *Atmos. Chem. Phys.*, 12, 11665-11678, 10.5194/acp-12-11665-2012, 2012.
- Hallquist, M., Wenger, J. C., Baltensperger, U., Rudich, Y., Simpson, D., Claeys, M., Dommen, J., Donahue, N. M., George, C., Goldstein, A. H., Hamilton, J. F., Herrmann, H., Hoffmann, T., Iinuma, Y., Jang, M., Jenkin, M. E., Jimenez, J. L., Kiendler-Scharr, A., Maenhaut, W., McFiggans, G., Mentel, T. F., Monod, A., Prevot, A. S. H., Seinfeld, J. H., Surratt, J. D., Szmigielski, R., and Wildt, J.: The formation, properties and impact of secondary organic aerosol: current and emerging issues, *Atmos. Chem. Phys.*, 9, 5155-5236, 2009.
- 30 Hansen, A. M. K., Kristensen, K., Nguyen, Q. T., Zare, A., Cozzi, F., Nojgaard, J. K., Skov, H., Brandt, J., Christensen, J. H., Strom, J., Tunved, P., Krejci, R., and Glasius, M.: Organosulfates and organic acids in Arctic aerosols: speciation, annual variation and concentration levels, *Atmos. Chem. Phys.*, 14, 7807-7823, 10.5194/acp-14-7807-2014, 2014.
- 35 Hansen, A. M. K., Hong, J., Raatikainen, T., Kristensen, K., Ylisirio, A., Virtanen, A., Petaja, T., Glasius, M., and Prisle, N. L.: Hygroscopic properties and cloud condensation nuclei activation of limonene-derived organosulfates and their mixtures with ammonium sulfate, *Atmos. Chem. Phys.*, 15, 14071-14089, 10.5194/acp-15-14071-2015, 2015.
- 40 Hatakeyama, S., Ohno, M., Weng, J. H., Takagi, H., and Akimoto, H.: Mechanism for the Formation of Gaseous and Particulate Products from Ozone-Cycloalkene Reactions in Air, *Environ. Sci. Technol.*, 21, 52-57, Doi 10.1021/Es00155a005, 1987.
- 45 Hettiyadura, A. P. S., Stone, E. A., Kundu, S., Baker, Z., Geddes, E., Richards, K., and Humphry, T.: Determination of atmospheric organosulfates using HILIC chromatography with MS detection, *Atmos. Meas. Tech.*, 8, 2347-2358, 10.5194/amt-8-2347-2015, 2015.
- Hyder, M., Genberg, J., Sandahl, M., Swietlicki, E., and Jonsson, J. A.: Yearly trend of dicarboxylic acids in organic aerosols from south of Sweden and source attribution, *Atmos. Environ.*, 57, 197-204, 10.1016/j.atmosenv.2012.04.027, 2012.
- 50 Iinuma, Y., Muller, C., Berndt, T., Boge, O., Claeys, M., and Herrmann, H.: Evidence for the existence of organosulfates from beta-pinene ozonolysis in ambient secondary organic aerosol, *Environ. Sci. Technol.*, 41, 6678-6683, 10.1021/es070938t, 2007.
- Jung, H. W., Tschaplinski, T. J., Wang, L., Glazebrook, J., and Greenberg, J. T.: Priming in Systemic Plant Immunity, *Science*, 324, 89-91, 10.1126/science.1170025, 2009.
- 55



- Kawamura, K., and Gagosian, R. B.: Implications of Omega-Oxocarboxylic Acids in the Remote Marine Atmosphere for Photooxidation of Unsaturated Fatty-Acids, *Nature*, 325, 330-332, Doi 10.1038/325330a0, 1987.
- 5 Kawamura, K., and Kaplan, I. R.: Motor Exhaust Emissions as a Primary Source for Dicarboxylic-Acids in Los-Angeles Ambient Air, *Environ. Sci. Technol.*, 21, 105-110, Doi 10.1021/Es00155a014, 1987.
- Kawamura, K., and Ikushima, K.: Seasonal-Changes in the Distribution of Dicarboxylic-Acids in the Urban Atmosphere, *Environ. Sci. Technol.*, 27, 2227-2235, Doi 10.1021/Es00047a033, 1993.
- 10 Kawamura, K., and Sakaguchi, F.: Molecular distributions of water soluble dicarboxylic acids in marine aerosols over the Pacific Ocean including tropics, *J. Geophys. Res.-Atmos.*, 104, 3501-3509, Doi 10.1029/1998jd100041, 1999.
- Kerminen, V. M.: Relative roles of secondary sulfate and organics in atmospheric cloud condensation nuclei production, *J. Geophys. Res.-Atmos.*, 106, 17321-17333, Doi 10.1029/2001jd900204, 2001.
- 15 Kristensen, K., and Glasius, M.: Organosulfates and oxidation products from biogenic hydrocarbons in fine aerosols from a forest in North West Europe during spring, *Atmos. Environ.*, 45, 4546-4556, 10.1016/j.atmosenv.2011.05.063, 2011.
- Kristensen, K.: Anthropogenic Enhancement of Biogenic Secondary Organic Aerosols - Investigation of Organosulfates and Dimers of Monoterpene Oxidation Products, Department of Chemistry and iNano, Aarhus University, Aarhus, Denmark, 2014.
- 20 Kristensson, A., Dal Maso, M., Swietlicki, E., Hussein, T., Zhou, J., Kerminen, V. M., and Kulmala, M.: Characterization of new particle formation events at a background site in Southern Sweden: relation to air mass history, *Tellus B*, 60, 330-344, 10.1111/j.1600-0889.2008.00345.x, 2008.
- 25 Kundu, S., Kawamura, K., Andreae, T. W., Hoffer, A., and Andreae, M. O.: Molecular distributions of dicarboxylic acids, ketocarboxylic acids and alpha-dicarbonyls in biomass burning aerosols: implications for photochemical production and degradation in smoke layers, *Atmos. Chem. Phys.*, 10, 2209-2225, 2010.
- 30 Laothawornkitkul, J., Taylor, J. E., Paul, N. D., and Hewitt, C. N.: Biogenic volatile organic compounds in the Earth system, *New Phytol.*, 183, 27-51, 10.1111/j.1469-8137.2009.02859.x, 2009.
- Ma, Y., Willcox, T. R., Russell, A. T., and Marston, G.: Pinic and pinonic acid formation in the reaction of ozone with alpha-pinene, *Chem. Commun.*, 1328-1330, 10.1039/b.617130c, 2007.
- 35 Mentel, T. F., Wildt, J., Kiendler-Scharr, A., Kleist, E., Tillmann, R., Dal Maso, M., Fisseha, R., Hohaus, T., Spahn, H., Uerlings, R., Wegener, R., Griffiths, P. T., Dinar, E., Rudich, Y., and Wahner, A.: Photochemical production of aerosols from real plant emissions, *Atmos. Chem. Phys.*, 9, 4387-4406, 2009.
- 40 Mochida, M., Kawabata, A., Kawamura, K., Hatsushika, H., and Yamazaki, K.: Seasonal variation and origins of dicarboxylic acids in the marine atmosphere over the western North Pacific, *J. Geophys. Res.-Atmos.*, 108, Artn 419310.1029/2002jd002355, 2003.
- Monson, R. K., Jones, R. T., Rosenstiel, T. N., and Schnitzler, J. P.: Why only some plants emit isoprene, *Plant Cell Environ.*, 36, 503-516, 10.1111/pce.12015, 2013.
- 45 Nguyen, Q. T., Christensen, M. K., Cozzi, F., Zare, A., Hansen, A. M. K., Kristensen, K., Tulinius, T. E., Madsen, H. H., Christensen, J. H., Brandt, J., Massling, A., Nojgaard, J. K., and Glasius, M.: Understanding the anthropogenic influence on formation of biogenic secondary organic aerosols in Denmark via analysis of organosulfates and related oxidation products, *Atmos. Chem. Phys.*, 14, 8961-8981, 10.5194/acp-14-8961-2014, 2014.
- 50 Olson, C. N., Galloway, M. M., Yu, G., Hedman, C. J., Lockett, M. R., Yoon, T., Stone, E. A., Smith, L. M., and Keutsch, F. N.: Hydroxycarboxylic Acid-Derived Organosulfates: Synthesis, Stability, and Quantification in Ambient Aerosol, *Environ. Sci. Technol.*, 45, 6468-6474, 10.1021/es201039p, 2011.
- 55 Penuelas, J., and Llusia, J.: BVOCs: plant defense against climate warming?, *Trends Plant Sci.*, 8, 105-109, 10.1016/S1360-1385(03)00008-6, 2003.



- 5 Pope, C. A., Thun, M. J., Namboodiri, M. M., Dockery, D. W., Evans, J. S., Speizer, F. E., and Heath, C. W.: Particulate Air-Pollution as a Predictor of Mortality in a Prospective-Study of Us Adults, *American Journal of Respiratory and Critical Care Medicine*, 151, 669-674, 1995.
- 10 Riva, M., Tomaz, S., Cui, T. Q., Lin, Y. H., Perraudin, E., Gold, A., Stone, E. A., Villenave, E., and Surratt, J. D.: Evidence for an Unrecognized Secondary Anthropogenic Source of Organosulfates and Sulfonates: Gas-Phase Oxidation of Polycyclic Aromatic Hydrocarbons in the Presence of Sulfate Aerosol, *Environ. Sci. Technol.*, 49, 6654-6664, 10.1021/acs.est.5b00836, 2015.
- 15 Schindelka, J., Iinuma, Y., Hoffmann, D., and Herrmann, H.: Sulfate radical-initiated formation of isoprene-derived organosulfates in atmospheric aerosols, *Faraday Discuss.*, 165, 237-259, 10.1039/c3fd00042g, 2013.
- 20 Seibert, P., and Frank, A.: Source-receptor matrix calculation with a Lagrangian particle dispersion model in backward mode, *Atmos. Chem. Phys.*, 4, 51-63, 2004.
- 25 Shalamzari, M. S., Ryabtsova, O., Kahnt, A., Vermeylen, R., Herent, M. F., Quetin-Leclercq, J., Van der Veken, P., Maenhaut, W., and Claeys, M.: Mass spectrometric characterization of organosulfates related to secondary organic aerosol from isoprene, *Rapid Commun. Mass Sp.*, 27, 784-794, 10.1002/rcm.6511, 2013.
- 30 Sharkey, T. D., Wiberley, A. E., and Donohue, A. R.: Isoprene emission from plants: Why and how, *Ann. Bot.-London*, 101, 5-18, 10.1093/aob/mcm240, 2008.
- 35 Stein, A. F., Draxler, R. R., Rolph, G. D., Stunder, B. J. B., Cohen, M. D., and Ngan, F.: NOAA's Hysplit Atmospheric Transport and Dispersion Modeling System, *B Am. Meteorol. Soc.*, 96, 2059-2077, 10.1175/Bams-D-14-00110.1, 2015.
- 40 Steinbrecher, R., Hauff, K., Hakola, H., and Rössler, J.: A revised parameterisation for emission modelling of isoprenoids for boreal plants., *Luxembourg*, 29-43, 1999.
- 45 Stephanou, E. G., and Stratigakis, N.: Oxocarboxylic and Alpha, Omega-Dicarboxylic Acids - Photooxidation Products of Biogenic Unsaturated Fatty-Acids Present in Urban Aerosols, *Environ. Sci. Technol.*, 27, 1403-1407, Doi 10.1021/Es00044a016, 1993.
- 50 Stohl, A., Forster, C., Frank, A., Seibert, P., and Wotawa, G.: Technical note: The Lagrangian particle dispersion model FLEXPART version 6.2, *Atmos. Chem. Phys.*, 5, 2461-2474, 2005.
- 55 Surratt, J. D., Kroll, J. H., Kleindienst, T. E., Edney, E. O., Claeys, M., Sorooshian, A., Ng, N. L., Offenberg, J. H., Lewandowski, M., Jaoui, M., Flagan, R. C., and Seinfeld, J. H.: Evidence for organosulfates in secondary organic aerosol, *Environ. Sci. Technol.*, 41, 517-527, 10.1021/es062081q, 2007a.
- Surratt, J. D., Lewandowski, M., Offenberg, J. H., Jaoui, M., Kleindienst, T. E., Edney, E. O., and Seinfeld, J. H.: Effect of acidity on secondary organic aerosol formation from isoprene, *Environ. Sci. Technol.*, 41, 5363-5369, 10.1021/es0704176, 2007b.
- 45 Surratt, J. D., Gomez-Gonzalez, Y., Chan, A. W. H., Vermeylen, R., Shahgholi, M., Kleindienst, T. E., Edney, E. O., Offenberg, J. H., Lewandowski, M., Jaoui, M., Maenhaut, W., Claeys, M., Flagan, R. C., and Seinfeld, J. H.: Organosulfate formation in biogenic secondary organic aerosol, *J. Phys. Chem. A*, 112, 8345-8378, 10.1021/jp802310p, 2008.
- 50 Surratt, J. D., Chan, A. W. H., Eddingsaas, N. C., Chan, M. N., Loza, C. L., Kwan, A. J., Hersey, S. P., Flagan, R. C., Wennberg, P. O., and Seinfeld, J. H.: Reactive intermediates revealed in secondary organic aerosol formation from isoprene, *P. Natl. Acad. Sci. USA*, 107, 6640-6645, 10.1073/pnas.0911114107, 2010.
- 55 Szmigielski, R., Surratt, J. D., Gomez-Gonzalez, Y., Van der Veken, P., Kourtchev, I., Vermeylen, R., Blockhuys, F., Jaoui, M., Kleindienst, T. E., Lewandowski, M., Offenberg, J. H., Edney, E. O., Seinfeld, J. H., Maenhaut, W., and Claeys, M.: 3-methyl-1,2,3-butanetricarboxylic acid: An atmospheric tracer for terpene secondary organic aerosol, *Geophys. Res. Lett.*, 34, ArtId L24811, 10.1029/2007gl031338, 2007.



Tolocka, M. P., and Turpin, B.: Contribution of Organosulfur Compounds to Organic Aerosol Mass, *Environ. Sci. Technol.*, 46, 7978-7983, 10.1021/es300651v, 2012.

5 Yttri, K. E., Simpson, D., Nojgaard, J. K., Kristensen, K., Genberg, J., Stenstrom, K., Swietlicki, E., Hillamo, R., Aurela, M., Bauer, H., Offenberg, J. H., Jaoui, M., Dye, C., Eckhardt, S., Burkhardt, J. F., Stohl, A., and Glasius, M.: Source apportionment of the summer time carbonaceous aerosol at Nordic rural background sites, *Atmos. Chem. Phys.*, 11, 13339-13357, 10.5194/acp-11-13339-2011, 2011.

10 Zhang, R. Y., Wang, L., Khalizov, A. F., Zhao, J., Zheng, J., McGraw, R. L., and Molina, L. T.: Formation of nanoparticles of blue haze enhanced by anthropogenic pollution, *P. Natl. Acad. Sci. USA*, 106, 17650-17654, 10.1073/pnas.0910125106, 2009.

Zhang, Y. Y., Muller, L., Winterhalter, R., Moortgat, G. K., Hoffmann, T., and Poschl, U.: Seasonal cycle and temperature dependence of pinene oxidation products, dicarboxylic acids and nitrophenols in fine and coarse air particulate matter, *Atmos. Chem. Phys.*, 10, 7859-7873, 10.5194/acp-10-7859-2010, 2010.

15



Table 1: Analyzed organic acids in the Vavihill aerosol samples. Measured m/z, molecular formula, possible molecular structure, suggested precursor and assigned precursor class. a) Hatakeyama et al. (1987), b) Stephanou and Stratigakis (1993), c) Kawamura and Gagosian (1987), d) Szmigielski et al. (2007), e) Ma et al. (2007), f) Claeys et al. (2009).

Precursor class	Name	Measured m/z	Molecular formula	Possible structure	Suggested precursor
Anthropogenic	Adipic acid	145.050	C ₆ H ₁₀ O ₄		Cyclohexene ^a
	Pimelic acid	159.065	C ₇ H ₁₂ O ₄		Cycloheptene ^a
Fatty acid-derived	Suberic acid	173.081	C ₈ H ₁₄ O ₄		Unsaturated fatty acid ^{b,c}
	Azelaic acid	187.097	C ₉ H ₁₆ O ₄		Unsaturated fatty acid ^{b,c}
1. generation Monoterpene	Pinic acid	185.081	C ₉ H ₁₄ O ₄		α-/β-pinene ^{d,e}
	Pinonic acid	183.102	C ₁₀ H ₁₆ O ₃		α-/β-pinene ^{d,e}
	Terpenylic acid	171.065	C ₈ H ₁₂ O ₄		α-pinene ^f
2. generation Monoterpene	3-methyl-1,2,3-butane-tricarboxylic acid (MBTCA)	203.055	C ₈ H ₁₂ O ₆		α-pinene ^d
	Diaterpenylic acid acetate (DTAA)	231.086	C ₁₀ H ₁₆ O ₆		α-pinene ^f



5

Table 2: Analyzed organosulfates (OSs) and nitrooxy organosulfates (NOSs) in the Vavihill aerosol samples. Measured m/z, molecular formula, possible molecular structure, suggested precursor and assigned precursor class. a) Surratt et al. (2007a), b) Schindelka et al. (2013), c) Olson et al. (2011), d) Shalamzari et al. (2013), e) Gomez-Gonzalez et al. (2008), f) Surratt et al. (Surratt et al., 2008), g) Hettiyadura et al. (2015), h) Surratt et al. (Surratt et al., 2010). The OSs and NOSs were quantified with D-mannose 6-sulfate (1), β -pinene OS 250 (2) or octyl sulfate (3).

Precursor class	Name	Measured m/z	Molecular formula	Possible structure	Suggested precursor
Isoprene/ Anthropogenic	OS 140 ¹	138.970	C ₂ H ₄ O ₅ S		Glycolaldehyde ^a
	OS 154 ¹	152.985	C ₃ H ₆ O ₅ S		Hydroxyacetone ^a /Methacrolein ^b / Methyl vinyl ketone ^b
	OS 156 ¹	154.961	C ₂ H ₄ O ₆ S		Glycolic acid ^{c,d} / Methyl vinyl ketone ^b
	OS 170 ¹	168.979	C ₃ H ₆ O ₆ S		Methylglycolic acid ^{c,d}
	OS 200 ¹	198.991	C ₄ H ₈ O ₇ S		2-methylglyceric acid ^{a,e}
Isoprene	OS 212 ¹	210.991	C ₅ H ₈ O ₇ S		Isoprene ^{f,g}
	OS 214 ¹	213.007	C ₅ H ₁₀ O ₇ S	 More isomers	Isoprene ^f
	OS 216 ¹	215.021	C ₅ H ₁₂ O ₇ S		C ₅ -epoxydiols from isoprene (IEPOX) ^h
Monoterpene	OS 250 ²	249.080	C ₁₀ H ₁₈ O ₅ S	 More isomers	α - β -pinene and limonene ^f
	OS 268 ²	267.053	C ₉ H ₁₆ O ₇ S		Limonene ^f
	OS 280 ²	279.054	C ₁₀ H ₁₆ O ₇ S		α - β -pinene ^f
Monoterpene NOS	NOS 295 ³	294.062	C ₁₀ H ₁₇ O ₇ NS	 More isomers	α - β -pinene, Limonene ^{a,f}
	NOS 297 ²	296.044	C ₉ H ₁₅ O ₈ NS	 More isomers	Limonene ^f



Table 3: Ranges of concentrations, means and standard deviation (SD) of the analyzed compounds in aerosol samples collected at the Vavihill measurement station 10th June to 18th of July 2012.

Compound	N	Minimum (ng/m ³)	Maximum (ng/m ³)	Mean (ng/m ³)	±SD (ng/m ³)
Adipic acid	36	0.03	19.27	1.76	3.87
Pimelic acid	36	0.02	1.21	0.38	0.28
Suberic acid	31	0.05	9.03	2.45	2.42
Azelaic acid	35	0.03	55.27	10.52	13.83
Pinic acid	38	0.28	4.71	1.31	1.04
Pinonic acid	38	0.82	10.66	2.89	2.00
Terpenylic acid	38	0.72	8.86	2.57	1.87
DTAA	38	0.04	5.67	0.84	1.23
MBTCA	38	0.38	29.42	6.18	7.00
OS 140	38	0.02	0.28	0.11	0.07
OS 154	38	0.15	2.95	0.76	0.64
OS 156	32	0.02	2.35	0.65	0.61
OS 170	38	0.08	0.78	0.33	0.17
OS 200	38	0.06	2.02	0.41	0.40
OS 212	38	0.16	4.63	0.91	0.95
OS 214	38	0.06	3.08	0.50	0.58
OS 216	38	0.06	5.83	0.63	1.07
OS 250	38	0.02	3.48	0.51	0.64
OS 268	38	0.01	0.48	0.13	0.12
OS 280	32	0.01	0.70	0.09	0.17
NOS 295	38	0.02	0.53	0.12	0.11
NOS 297	37	0.01	0.18	0.05	0.03



Table 4: Correlation matrix displaying the Pearson product-moment coefficient (r) for measured chemical species. Colours represent degree of correlation: yellow: $[0.7-0.8]$; green: $[0.8-0.9]$; red: $[0.9-1.0]$.

	Adipic acid	Pimelic acid	Suberic acid	Azelaic acid	Pinic acid	Pinonic acid	Terpenylic acid	DTAA	MBTCA	OS 140	OS 154	OS 156	OS 170	OS 200	OS 212	OS 214	OS 216	OS 250	OS 268	OS 280	NOS 295	NOS 297	
Adipic acid	0.16																						
Pimelic acid	0.02	0.95																					
Suberic acid	0.02	0.95	0.95																				
Azelaic acid	0.01	0.87	0.95	0.95																			
Pinic acid	0.25	0.20	0.01	0.20	0.81																		
Pinonic acid	0.05	0.02	0.32	0.00	0.81	0.81																	
Terpenylic acid	0.33	0.35	0.18	0.40	0.80	0.39	0.89																
DTAA	0.35	0.29	0.18	0.37	0.66	0.20	0.89	0.94	0.92														
MBTCA	0.32	0.22	0.06	0.26	0.71	0.29	0.94	0.92	0.93	0.70													
OS 140	0.13	0.41	0.27	0.50	0.47	0.06	0.90	0.83	0.70	0.82													
OS 154	0.33	0.36	0.22	0.43	0.67	0.19	0.92	0.94	0.93	0.82	0.82												
OS 156	0.22	0.36	0.26	0.34	0.62	0.21	0.83	0.87	0.84	0.76	0.92	0.92											
OS 170	0.24	0.24	0.00	0.31	0.58	0.21	0.77	0.73	0.80	0.84	0.86	0.83	0.84										
OS 200	0.27	0.32	0.19	0.41	0.58	0.10	0.81	0.93	0.86	0.80	0.96	0.93	0.84	0.98									
OS 212	0.34	0.35	0.22	0.43	0.65	0.17	0.86	0.97	0.88	0.76	0.97	0.92	0.81	0.98	0.98								
OS 214	0.33	0.30	0.18	0.38	0.61	0.15	0.80	0.96	0.82	0.70	0.92	0.89	0.74	0.97	0.98	0.98							
OS 216	0.33	0.26	0.21	0.33	0.50	0.06	0.65	0.89	0.68	0.55	0.80	0.79	0.57	0.89	0.91	0.96	0.96						
OS 250	0.20	0.00	0.00	0.00	0.48	0.26	0.56	0.45	0.51	0.51	0.54	0.59	0.63	0.53	0.50	0.45	0.31	0.45	0.31				
OS 268	0.19	0.12	0.00	0.08	0.63	0.36	0.80	0.72	0.87	0.63	0.78	0.67	0.72	0.71	0.69	0.64	0.45	0.55	0.55	0.75			
OS 280	0.38	0.24	0.15	0.14	0.56	0.08	0.84	0.83	0.93	0.65	0.88	0.77	0.76	0.78	0.82	0.75	0.66	0.39	0.39	0.75	0.55		
NOS 295	0.00	0.00	0.00	0.00	0.56	0.56	0.53	0.38	0.62	0.35	0.44	0.44	0.50	0.32	0.33	0.27	0.09	0.33	0.33	0.70	0.55		
NOS 297	0.01	0.14	0.00	0.14	0.53	0.35	0.67	0.57	0.77	0.57	0.68	0.61	0.68	0.59	0.57	0.50	0.31	0.42	0.42	0.85	0.70	0.88	



Table 5: Ranges, means and standard deviations (SD) of the FLEXPART surface type exposure of incoming air masses during 10th June to 18th of July 2012.

Surface type	N	Minimum (%)	Maximum (%)	Mean (%)	±SD (%)
Pasture	38	0	13	4.4	3.6
Discontinuous urban fabric	38	1	7	2.6	1.7
Non-irrigated arable land	38	7	35	18.8	8.3
Sparsely vegetated areas	38	0	3	0.4	0.9
Broad leaved forest	38	0	8	2.6	1.7
Lakes and ponds	38	0	3	0.9	0.6
Moors and heath	38	0	3	0.5	0.7
Coniferous forest	38	0	22	5.5	5.2
Sea and ocean	38	24.6	86	56.0	16.3
Other	38	3	15	8.3	3.2



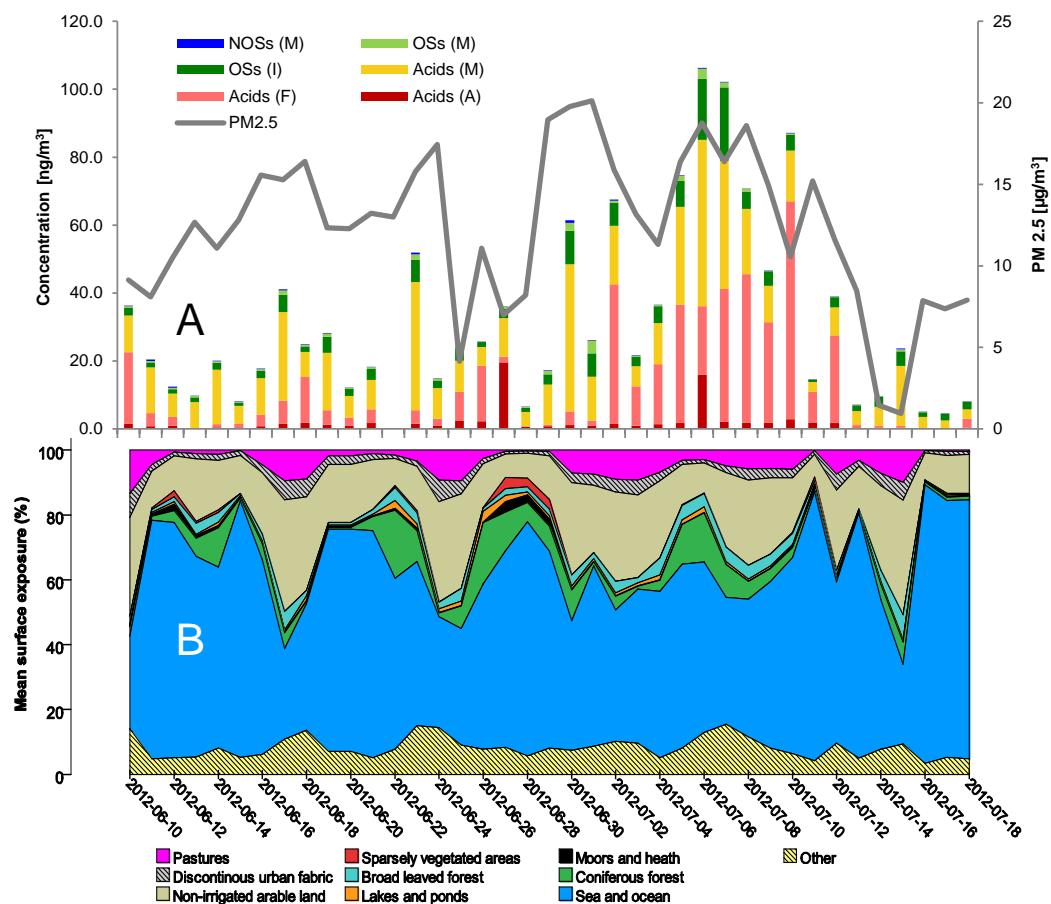
Table 6: Correlation matrix displaying the Pearson product-moment coefficient (r) for surface types. Colours represent degree of correlation: yellow: $|0.7-0.8|$; green: $|0.8-0.9|$; red: $|0.9-1.0|$.

	Pasture	Discontinuous urban fabric	Non-irrigated arable land	Sparsely vegetated areas	Broad leaved forest	Lakes and ponds	Moors and heath	Coniferous forest	Sea and ocean	Other
Pasture										
Discontinuous urban fabric	0.92									
Non-irrigated arable land	0.89	0.9								
Sparsely vegetated areas	-0.47	-0.42	-0.49							
Broad leaved forest	0.48	0.32	0.53	-0.13						
Lakes and ponds	0	-0.12	-0.13	0.18	0.2					
Moors and heath	-0.46	-0.4	-0.47	0.98	-0.17	0.14				
Coniferous forest	-0.17	-0.31	-0.22	0.23	0.43	0.8	0.17			
Sea and ocean	-0.84	-0.78	-0.84	0.27	-0.73	-0.31	0.28	-0.28		
Other	0.59	0.57	0.53	-0.16	0.42	0.29	-0.18	0.23	-0.77	

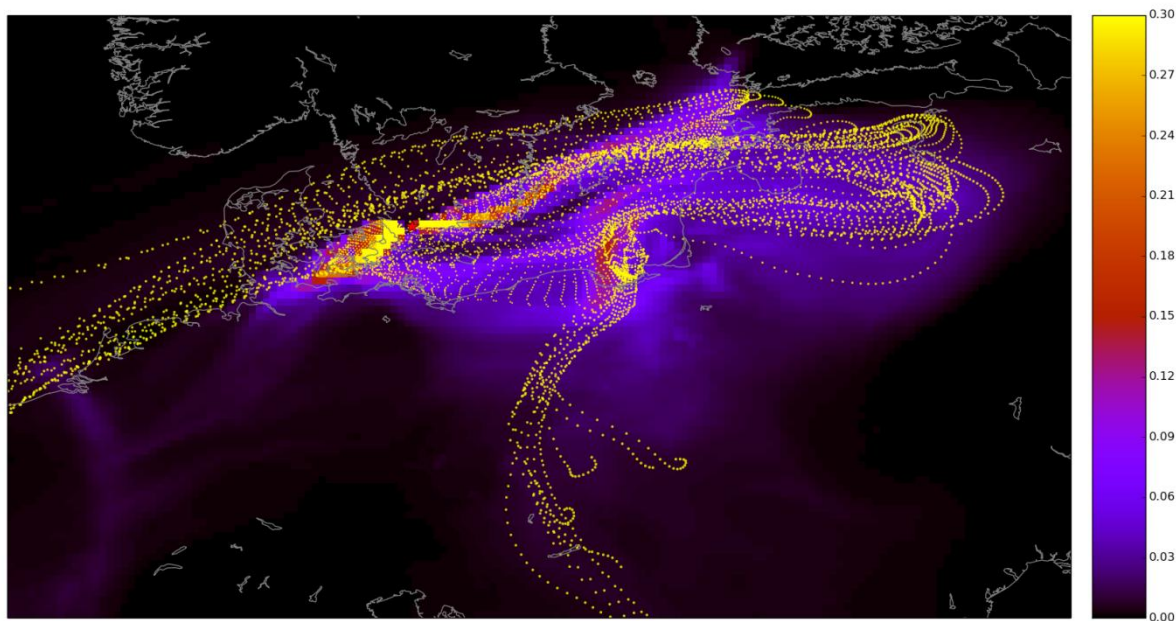


Table 7: Principal component (PC) loadings. The loadings display the variation (between -1 and 1) explained by the PC. Numbers in bold indicates absolute number >0.6. PC1 explained 49.1%, PC2 14.9%, PC3 9.3% and PC4 6.9%.

	Principal Component			
	1	2	3	4
Adipic acid	0.37	-0.25	0.08	0.59
Pimelic acid	0.24	0.20	0.75	-0.21
Suberic acid	0.20	0.26	0.82	-0.19
Azelaic acid	0.21	0.39	0.74	-0.17
Pinic acid	0.70	-0.04	-0.25	0.14
Pinonic acid	0.19	-0.15	-0.37	0.16
Terpenylic acid	0.88	0.29	-0.11	0.04
DTAA	0.93	0.24	0.04	0.09
MBTCA	0.89	0.28	-0.26	-0.02
OS 140	0.76	0.30	0.12	-0.41
OS 154	0.96	0.22	0.04	-0.10
OS 156	0.93	0.06	0.04	-0.14
OS 170	0.79	0.20	-0.17	-0.28
OS 200	0.92	0.18	0.10	-0.12
OS 212	0.95	0.18	0.13	-0.01
OS 214	0.92	0.13	0.15	0.04
OS 216	0.87	0.03	0.26	0.11
OS 250	0.48	-0.06	-0.38	-0.06
OS 268	0.67	0.24	-0.51	-0.18
OS 280	0.87	0.13	-0.20	-0.05
NOS 295	0.43	0.16	-0.69	-0.25
NOS 297	0.59	0.28	-0.48	-0.35
Pastures	0.22	0.85	0.15	-0.37
Discontinuous urban fabric	-0.02	0.92	0.12	-0.29
Non-irrigated arable land	0.20	0.94	0.10	-0.14
Broad leaved forest	0.53	0.77	0.21	0.11
Sparsely vegetated areas	-0.11	-0.10	-0.18	0.86
Lakes and ponds	0.76	0.34	0.02	0.42
Moors and heath	-0.16	-0.04	-0.23	0.85
Coniferous forest	0.79	0.35	-0.04	0.39
Sea and ocean	0.37	0.62	0.27	0.34
Other	0.60	0.65	0.19	0.19



5 Figure 1: A) Total concentration of all measured carboxylic acids, organosulfates (OSs) and nitrooxy organosulfates (NOSs) in PM_1 collected at the Vavihill measurement station. The thick grey line displays the $\text{PM}_{2.5}$ concentration. Capital letters in parenthesis in the legend is the precursor class given in Table 1 and 2. A=Anthropogenic, F=Fatty acid, I=Isoprene and M=Monoterpenes. B) FLEXPART generated mean exposure from the nine mean largest surface categories. The exposure is a mean of 3, 5 and 7 days back trajectories. The category “Other” represents the remaining 34 surface categories. More detailed information on the surface categories can be found in the supplemental information.



5 **Figure 2:** 120 hour back-trajectory air mass covering the concentration peak dates; 6-8th July. FLEXPART are shown in shaded colors while HYSPLIT are displayed by yellow dotted trajectories. The dots size increase with the air mass age. The colorbar displays the FLEXPART footprint, normalized to 1 (the color range has been limited to 0-0.3 to highlight grid points with low but a non-zero contribution). Together, the grid points with a value larger than 0.1 contribute 17% of the total sensitivity while grid boxes with a value larger than 0.01 contribute 81% of the total sensitivity. 120 h back-trajectory was chosen for easier interpretation of the illustration.